https://doi.org/10.2478/acph-2025-0025

Original research paper

Scutellarin mitigates LPS-ATP-induced cardiomyocyte pyroptosis through the inhibition of the NLRP3/caspase-1/GSDMD signaling pathway

XIAO-WEI LI[1#]
YUN-FEI CHEN[1#]
LAN ZHOU[2]
PENG ZHOU[2]
PENG HUANG[2]
QIAN NIU[3*]
JIN-CAI LI[4*]

[1] *Pharmacy Department, Mengcheng Hospital of Traditional Chinese Medicine, Mengcheng, Anhui, 233500, China*

[2] *Department of Integrated Traditional Chinese and Western Medicine, Anhui University of Chinese Medicine, Hefei, Anhui, 230012, China*

[3] *Department of Pharmacy, Bozhou Vocational and Technical College, Bozhou, Anhui, 236800, China*

[4] *School of Traditional Chinese Medicine, Bozhou University, Bozhou, Anhui, 236800, China*

[a] These authors contributed equally to this work.

[*] Correspondence to: ahniuqian@bzy.edu.cn; ahbanli@bzuu.edu.cn

ABSTRACT

Scutellarin has a good myocardial protective effect. However, the underlying mechanism of scutellarin on cardiomyocyte pyroptosis remains unclear. In this study, we elucidated the mechanism of scutellarin to protect the injured myocardium. The molecular docking technique was used to predict the targets of scutellarin in protecting against myocardial injury. H9c2 cell pyroptosis was induced by lipopolysaccharide (LPS) and adenosine triphosphate (ATP). Then, the activities of CK and LDH were measured through a colorimetric assay. The level of cTnI was quantified by ELISA. mRNA expressions of NLRP3, cysteine-dependent aspartate-specific protease-1 (caspase-1), gasdermin D (GSDMD), interleukin-1β (IL-1β), and interleukin-18 (IL-18) were analyzed using RT-qPCR. Protein expressions of NLRP3, caspase-1, and GSDMD were detected by immunofluorescence technique. Protein expressions of NLRP3 was analyzed using Western blotting. Scutellarin had a good binding

affinity with NLRP3, caspase-1, and GSDMD. Compared with LSP and ATP-treated cells, concentrations of 25, 50, and 100 μmol/L scutellarin reduced CK and LDH activities and the level of cTnI, decreased the expression of the mRNA expressions of NLRP3, caspase-1, and GSDMD. In the mechanism study, scutellarin decreased mRNA expressions of NLRP3, caspase-1, GSDMD, IL-1β, and IL-18, and reduced the fluorescence expressions of NLRP3, caspase-1, and GSDMD. Scutellarin reduced the protein expression of NLRP3. Scutellarin inhibits myocardial cell pyroptosis induced by LPS and ATP, and the mechanism is related to the NLRP3/caspase-1/GSDMD signaling pathway.
Keywords: scutellarin, LPS, ATP, NLRP3/caspase-1/GSDMD signaling pathway

Accepted June 24, 2025
Published online June 24, 2025

INTRODUCTION

The nucleotide-binding domain and leucine-rich repeat protein 3 (NLRP3) inflammasome is a new target in cardiovascular disease (CVD) treatment (1). NLRP3 inflammasome infiltration has been identified to play a central role in the pathological progression of vascular damage spanning atherosclerosis, aneurysm, ischemic heart disease, and other nonischemic heart diseases including diabetic cardiomyopathy, chronic heart failure, and hypertension- or virus-induced cardiac dysfunction (2–5). Therefore, the inhibition of NLRP3 inflammasome may help in the prevention or treatment of CVD.

The NLRP3 inflammasome, a key participant in the innate immune response, requires both priming and activation signals for the initiation of inflammation (6). NLRP3 iflammasome is composed of NLRP3, ASC (apoptosis-associated speck-like protein containing a caspase recruitment domain (CARD)), and caspase-1 (cysteine-dependent aspartate-specific protease-1), the assembly of which promotes the activation of caspase-1 and the maturation and secretion of inflammatory cytokines (i.e., interleukin-1β (IL-1β), IL-18 or could cause pyroptosis, an identified pathway of programmed cell death (7).

Scutellarin (4,5,6-trihydroxyflavone7-glucuronide) is a bioactive flavonoid extracted from Erigeron plants, Scutellaria plants, Opuntia plants, Centaurus plants, and Anaphalis plants (8, 9). Scutellarin shows various pharmacological properties on antioxidation and anti-inflammation in the treatment of CVD, including alleviating cardiac fibrosis and decreasing the infarct size and dysfunction of rats with myocardial ischemia, suppressing cardiac hypertrophy, protecting against doxorubicin-induced acute cardiotoxicity (10). In a myocardial ischemia-reperfusion injury rat model, scutellarin significantly improved cardiac diastolic dysfunction and myocardial structural abnormalities, and inhibited NLRP3 inflammasome activation (11). Therefore, scutellarin has a myocardial protective effect, and

its mechanism is related to its inhibitory activity of NLRP3. However, it is unclear whether scutellarin can inhibit cell pyroptosis induced by lipopolysaccharide (LPS) and adenosine triphosphate (ATP), therefore, the mechanism of myocardial protection of scutellarin can be clarified. In this study, LPS and ATP-induced pyroptosis model was used to explore further the relationship between the protective effect of scutellarin on H9c2 rat cardiomyocytes and the NLRP3/caspase-1/GSDMD signaling pathway.

EXPERIMENTAL

Drugs and reagents

Scutellarin (B21478, purity≥98 %) was purchased from Shanghai Yuanye Biotechnology Co., Ltd., China. LPS (L8880) was purchased from Beijing Solarbio Science & Technology Co., Ltd., Beijing, China. ATP (A832633) was purchased from Shanghai Macklin Biochemical Co., Ltd., China. Trizol (G3013), SYBR (G3326-15), and Alexa Fluor® 488-conjugated Goat Anti-Rabbit IgG were purchased from Wuhan Servicevbio Biotechnology Co., Ltd., China. Reagent for determination of cardiac troponin I (cTnI, MM-0426R1) concentration was bought from Meimian, China. The reagents for determination of lactate dehydrogenase (LDH, A020-2-2) and creatine kinase (CK, A032-1-1) activities were purchased from Nanjing Jiancheng Bioengineering Insitute, Nanjing, China. Anti-glyceraldehyde-3-phosphatedehydrogenase (GAPDH) (A19056) was purchased from ABclonal. Anti-NLRP3 (AB263899) and anti-GSDMD (anti-gasdermin D) (ab219800) were purchased from Abcam. H9c2 cells were purchased from Wuhan Pricella Biotechnology Co., Ltd., China. Dulbecco's Modified Eagle Medium (DMEM, BL304A), fetal bovine serum (FBS, BL201A), penicillin streptomycin solution (P/S, BL505A), and pancreatic enzyme (BL501A) were purchased from Biosharp, Shanghai, China. Primers for mRNA expressions of NLRP3, caspase-1, GSDMD, IL-1β, and IL-18 were purchased from Sangon Biotech, China.

Molecular docking

The chemical structure of scutellarin was downloaded from the PubChem database (https://pubchem.ncbi.nlm.nih.gov/), subjected to energy optimization and hydrogenation using Chem3D software (https://softwaretopic.informer.com/chem3d-free-software/). “NLRP3 (6npy) (12)”, “caspase-1 (1rwx) (13)” and “GSDMD (5wqt) (14)” were downloaded from the RCSB protein database (https://www.rcsb.org/). Molecular docking was performed using the CB-DOCK2 platform (https://cadd.labshare.cn/cb-dock2/php/index.php) (15).

In vitro *study*

Cell culture and grouping. – Rat cardiomyocyte H9c2 is a subclonal cell line derived from the

cardiac tissue of BD1X rats during the embryonic stage. H9c2 cells were cultured in a 5 % CO_2 incubator at 37 °C with Dulbecco's Modified Eagle Medium (DMEM) supplemented with 10 % fetal bovine serum (FBS) and 1 % penicillin-streptomycin solution. When the H9c2 cell density reached 85–90 %, the cells were digested with pancreatic enzyme, and the cells (2×10^5) were inoculated in 6-well or 96-well plates for follow-up experiments. While examining the cell pharmacodynamics, H9c2 cells were divided into the control group (complete medium culture), model group (treated with 10 μg mL^{-1} LPS for 12 h and with 8 mM ATP for the next 2 h), 25 μmol L^{-1} scutellarin group (25 group), 50 μmol L^{-1} scutellarin group (50 group), and 100 μmol L^{-1} scutellarin group (100 group). Each of these three scutellarin groups was first pre-treated with scutellarin (25, 50 or 100 μmol L^{-1}) for 12 h, afterwards cells were incubated with 10 μg mL^{-1} LPS for 12 h and subsequently with 8 mmol L^{-1} ATP for the next 2 h (16, 17). During the cellular mechanistic studies, H9c2 cells were divided into the control group (complete medium culture), model group (treated with 10 μg mL^{-1} LPS for 12 h and with 8 mmol L^{-1} ATP for the next 2 h), and scutellarin group (after pre-treatment with 25 μmol L^{-1} scutellarin for 12 h, cells were further incubated with 10 μg mL^{-1} LPS for 12 h and subsequently with 8 mmol L^{-1} ATP for the next 2 h).

Detection of LDH, CK, and cTnI. – H9c2 cells were crushed by ultrasound, cell culture medium was collected, and cell supernatant was obtained by centrifugation. LDH and CK activities were assesed according to the kit instructions using a microplate reader (Peiou Analytical Instrument Co., LTD). The level of cTnI in the supernatant from H9c2 cells was assessed following the instructions provided by the enzyme-linked immunosorbent assay (ELISA) kit using a microplate reader.

Immunofluorescence staining for detection of proteins. – H9c2 cells were fixed with 4 % paraformaldehyde for 20 min, permeabilized with 0.5 % Triton X-100 for 20 min, and blocked at room temperature using 10 % goat serum for 1 h. Following blocking, the goat serum was discarded, and the cells were incubated overnight at 4°C with antibodies against NLRP3 (1:200, in PBS), caspase-1 (1:200, in PBS), and GSDMD (1:200, in PBS), respectively. On the second day, the primary antibody was removed, and the samples were incubated with Alexa Fluor® 488-conjugated Goat Anti-Rabbit IgG (1:200, in PBS) at room temperature for 1 h. Subsequently, DAPI (4',6-diamidino-2-phenylindole) was applied for 5 min at room temperature before observation under an inverted fluorescence microscope (Olympus BX81, Japan). Immunofluorescence quantification was conducted using ImageJ software (https://imagej.net/ij/index.html).

RT- qPCR for detection of mRNA expression. – Total RNA was extracted using a Trizol

reagent. Subsequently, the RNA concentration was measured with an Eppendorf BioPhotometer Plus, and its purity was assessed by evaluating absorbance at 260 nm and 280 nm. The RNA was then reverse transcribed into cDNA utilizing a Mastercycler® nexus gradient (Germany). The cDNA was subsequently subjected to real-time fluorescence quantification utilizing a LightCycler® 96 PCR instrument (Roche, Switzerland). The amplification procedure consisted of pre-denaturation at 95 ℃ for 5 min, denaturation at 95 °C for 15 s, annealing at 60 °C for 60 s, and PCR at 40 cycles. The melting curve analysis was conducted within the temperature range of 60 to 95 °C. The results were analyzed using β-actin as a control, employing the $2^{-\Delta\Delta Cq}$ method to evaluate the mRNA levels of NLRP3, caspase-1, GSDMD, IL-1β, and IL-18. The primers utilized in this study are detailed in Table I.

Table I. Sequence of primers

Primers		Sequence (5' →3')
NLRP3	Forward	5′-GAGCTGGACCTCAGTGACAATGC-3′
	Reverse	5′-AGAACCAATGCGAGATCCTGACAAC-3′
Caspase-1	Forward	5′-GCACAAGACTTCTGACAGTACCTTCC-3′
	Reverse	5′-GCTTGGGCACTTCAATGTGTTCATC-3′
GSDMD	Forward	5′-CAGCAGGCAGCATCCTTGAGTG-3′
	Reverse	5′-CCTCCAGAGCCTTAGTAGCCAGTAG-3′
IL-1β	Forward	5’-AATCTCACAGCAGCATCTCGACAAG -3’
	Reverse	5’-TCCACGGGCAAGACATAGGTAGC -3’
IL-18	Forward	5’-CGACCGAACAGCCAACGAATCC -3’
	Reverse	5’-GTCACAGCCAGTCCTCTTACTTCAC -3’
β-actin	Forward	5′-CCCATCTATGAGGGTTACGC-3′
	Reverse	5′-TTTAATGTCACGCACGATTTC-3′

Western blot for detection of protein expression

H9c2 cells were harvested and lysed using RIPA lysis buffer. The resulting homogenate was centrifuged at 13684 × g for 10 min at 4 ℃. Total protein was separated using 12 % sodium dodecyl sulfate-polyacrylamide gel electrophoresis (SDS-PAGE) and transferred to polyvinylidene fluoride (PVDF) membrane. The membrane was blocked with 5 % free-fat milk for 1 h at room temperature, and then incubated with NLRP3 (1:1000) and GAPDH (1:5000) at 4 ℃ overnight. After washing the membranes three times with tris buffered saline with Tris-buffered saline with Tween (TBST), they were incubated with secondary antibodies (Goat Anti-Rabbit IgG, 1:10000) for 2 h. Electrochemiluminescence (ECL) was employed to

assess the density of protein bands, and imaging was conducted using the Tanon5200 system (Tanon, China) to capture photographs of the protein bands.

Statistical analysis

The data were presented as mean ± standard deviation (SD), and SPSS 26.0 was used for statistical analysis. One-way ANOVA was used to determine the difference. $p < 0.05$ was considered statistically significant.

RESULTS AND DISCUSSION

Molecular docking results

Previous evidence suggests that NLRP3 inflammasome plays an important role in the pathogenesis of CVDs, including myocardial infarction, myocardial ischemia-reperfusion injury, heart failure, atrial fibrillation, and hypertension (4). The NLRP3 inflammasome is a macromolecular polyprotein complex that can be activated by endogenous risk signals and exogenous factors (18). After activation of NLRP3, ASC and pro-caspase-1 can be recruited, and then caspase-1 can be activated to promote the maturation and secretion of IL-1β and IL-18 (19). In addition, caspase-1 also cleaves GSDMD to form N-terminal products, which then form pores in the plasma membrane to mediate pyroptosis (20). Recently studies showed that plasma caspase-1 and IL-1β levels were significantly elevated at autopsy in patients with acute myocardial infarction (AMI) (21). ASC expression was increased in infiltrating cells, especially macrophages and neutrophils, in the heart tissue of patients with AMI (22). A lack of NLRP3 inflammasome can reduce inflammation and promote cardiac protection (23). These results suggested that the NLRP3 inflammasome is closely involved in the pathogenesis of cardiovascular diseases (myocardial infarction, heart failure, *etc.*). Therefore, the development of drugs that inhibit the NLRP3 signaling pathway is particularly important to mitigate the progression of CVDs. In this study, molecular docking was used to detect the binding affinity of scutellarin with NLRP3, caspase-1, and GSDMD. The binding energy scores of scutellarin with NLRP3, caspase-1 and GSDMD were –9.9, –8.4 and –6.5 kcal mol^{-1} respectively, all lower than –5 kcal mol^{-1}, and were considered to indicate that the binding results were relatively stable (Table II, Fig. 1), which may exert inhibition of the NLRP3/caspase-1/GSDMD signaling pathway. Then, the *in vitro* experiments were used to verify the docking results.

Table II. Docking results of scutellarin with NLRP3, caspase-1, and GSDMD

Target	Vina Score (kcal/mol)	Cavity score	Center (x, y, z)	Size (x, y, z)	Amino acid residue

NLRP3	-9.9	2121 7	98, 95, 104	35, 35, 35	Val351, Leu632, Met635,Gln636, Glu637, Glu638, Asp639, Phe640, Val641, Gln642, Arg643, Ala644, Met645, Tyr647, Glu693, Lys694, Glu695, Gly696, Arg697, His698, Leu699, Asp700, Met701, Val702, Leu718, Asn720, Asp745
Caspase-1	-8.4	623	41, 65, 7	24, 24, 24	Trp340, Arg341, His342, Pro343, Thr344, Met345, Gly346, Ser347, Val348, Phe349, Ile350, Gly351, Arg352, Glu355, Ser276, Phe377, Glu378, Gln379, Pro380, Asp381, Gly382, Arg383, Ala384, Gln385
GSDMD	-6.5	963	30, -82, 41	24, 24, 24	Ala53, Glu56, Ala57, Leu58, Glu59, Glu68, Pro69, Leu70, Asp71, Leu78, Ala82, Gly86, Leu88, Val89, Pro90, Ala93, Ile94, Val97

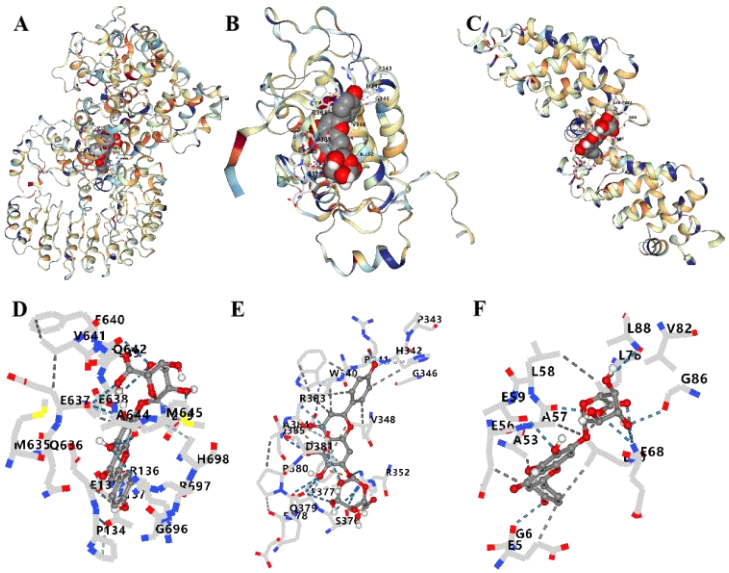

Fig. 1. The docking pictures of scutellarin with NLRP3, caspase-1, and GSDMD: a) 3D diagram of scutellarin-NLRP3; b) 3D diagram of scutellarin-caspase-1; c) 3D diagram of scutellarin-GSDMD; d) amino acid residue of scutellarin-NLRP3; e) amino acid residue of scutellarin-caspase-1; f) amino acid residue of scutellarin-GSDMD.

Effect of scutellarin on the activities of CK and LDH, and level of cTnI in LPS and ATP-induced pyroptosis model cells

LDH is a widely recognized marker utilized for evaluating cellular activity and as an

indicator of cardiomyocyte injury. CK is an important indicator of myocardial infarction. cTnI is a biomarker of myocardial injury and a preferred blood test indicator for patients with AMI. Therefore, these indicators can be regarded as important indicators of myocardial injury. Compared with the control group, the CK and LDH activities, and the level of cTnI in the model group were significantly increased (P<0.01). Compared with the model group, 25, 50, 100 μmol/L scutellarin reduced CK and LDH activities, as well as the level of cTnI (P<0.05, P<0.01) (Fig **2**). These results indicated that scutellarin could significantly reduce myocardial injury indexes.

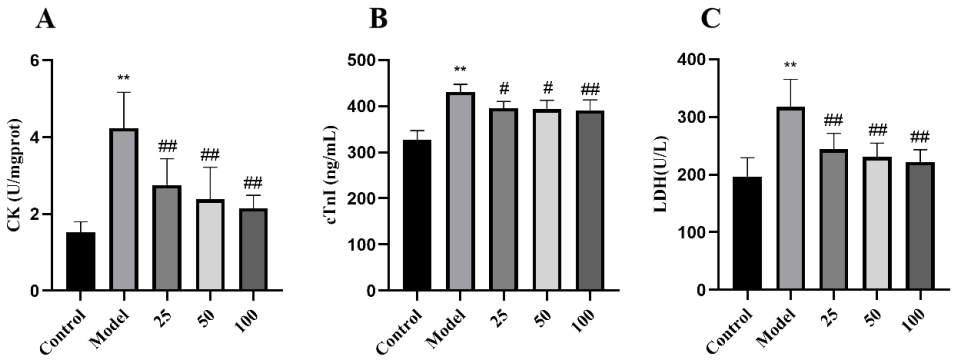

Fig. 2. Effect of scutellarin on CK and LDH activities, and the level of cTnI in LPS and ATP-induced pyroptosis model cells: a) CK; b) cTnI, c) LDH. 25 group: 25 μmol L^{-1} scutellarin group, 50 group: 50 μmol L^{-1} scutellarin group, 100 group: 100 μmol L^{-1} scutellarin group. Data are presented as mean ± SD (n = 6). Compared with control group, $^{**}p$ < 0.01; compared with model group, $^{\#}p$ < 0.05, $^{\#\#}p$ < 0.01.

Effect of different doses of scutellarin on the mRNA expressions of NLRP3, caspase-1, and GSDMD in LPS and ATP-induced pyroptosis model cells

At present, LPS combined with ATP is a common method for pyroptosis models *in vitro* (24). As a component of the outer wall of bacteria, LPS can activate immune cells through the signal transduction system, release a variety of inflammatory mediators, and induce inflammation (25). ATP is an energy storage substance and an important endogenous signaling molecule for inflammation (26). LPS and ATP can activate the classical pyroptosis pathway mediated by NLRP3 inflammasome (17). In this study, LPS and ATP increased the mRNA expressions of NLRP3, caspase-1, and GSDMD in the model group as compared to the control group (p < 0.01). Compared with the model group, 25, 50, and 100 μmol L^{-1} scutellarin decreased the expression of these mRNA expressions (p < 0.05, p < 0.01) (Fig. 3). Thus, the prevention of cardiomyocyte injury by scutellarin might be related to the inhibition of the NLRP3/caspase-1/GSDMD signaling pathway.

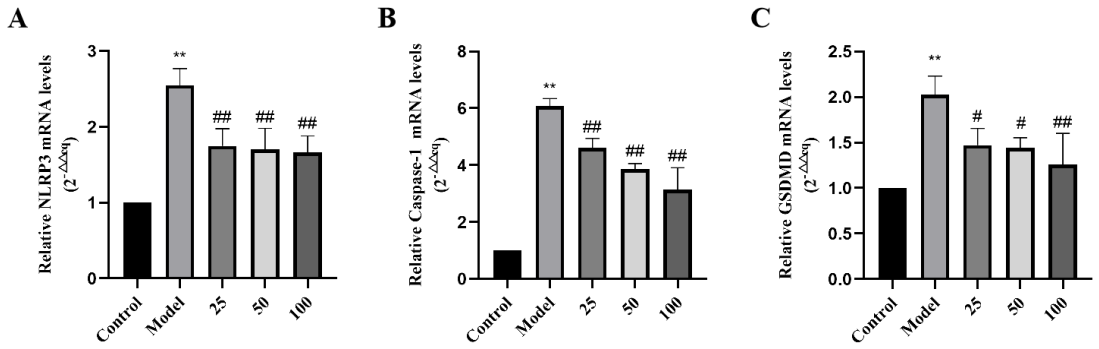

Fig. 3. Effect of different doses of scutellarin on the mRNA expression of NLRP3, caspase-1, and GSDMD in LPS and ATP-induced pyroptosis model cells: a) NLRP3 mRNA; b) caspase-1 mRNA; c) GSDMD mRNA. 25 group: 25 μmol L^{-1} scutellarin group, 50 group: 50 μmol L^{-1} scutellarin group, 100 group: 100 μmol L^{-1} scutellarin group. Data are presented as mean ± SD (n = 3). Compared with control group, $^{**}p < 0.01$, Compared with model group, $^{\#}p < 0.05$, $^{\#\#}p < 0.01$.

Effect of scutellarin on the key mRNA expression of the NLRP3/caspase-1/GSDMD signaling pathway in LPS and ATP-induced pyroptosis model cells

Scutellarin slowed the heart rate, regulated myocardial contractility, reduced cardiac preload and afterload, and increased myocardial oxygen supply, which has been widely used in the clinical treatment of cardiovascular diseases (27). Scutellarin mediates ischemia/reperfusion-induced cardiomyocyte apoptosis and cardiac dysfunction by regulating the activation of the Bcl-2/Bax/Caspase-3 signaling pathway via the cGAS-STING signaling pathway (28). Scutellarin could improve oxidative stress, inflammation, and reduce apoptosis by modulating NRF2/KEAP/ARE, TLR4/MYD88/NF-κB, and apoptosis pathways to treat and prevent myocardial injury complicated by type 2 diabetes mellitus (29). Scutellarin can also inhibit NLRP3 overexpression, which is mainly reflected in decreasing p-p65/p65 ratio, IκBα degradation, and levels of NLRP3, caspase-1, ASC, GSDMD-N, IL-1β, and IL-18, which ameliorated pulmonary fibrosis through inhibiting NF-κB/NLRP3-mediated epithelial-mesenchymal transition and inflammation (30). Scutellarin attenuated oleic acid-induced vascular smooth muscle foam cell formation via the suppression of NLRP3 inflammasome activation (31). Scutellarin inhibited the activation of the NF-κB and MAPK signaling pathways, as well as the activity of the NLRP3 inflammasome caused by TNF-α. This could potentially aid in the treatment of intervertebral disc degeneration (32). Scutellarin effectively improved LPS-induced inflammation-related depressive-like behaviors via the regulation of the ROS/NLRP3 signaling pathway and microglia activation (33). Scutellarin has a good myocardial protective effect, and it can also inhibit NLRP3 inflammasome activation, which provides a theoretical basis for this study. In this paper, compared with the

control group, mRNA expressions of NLRP3, caspase-1, GSDMD, IL-1β, and IL-18 in the model group were increased ($p < 0.01$). Compared with the model group, scutellarin reversed these mRNA expressions ($p < 0.01$) (Fig. 4).

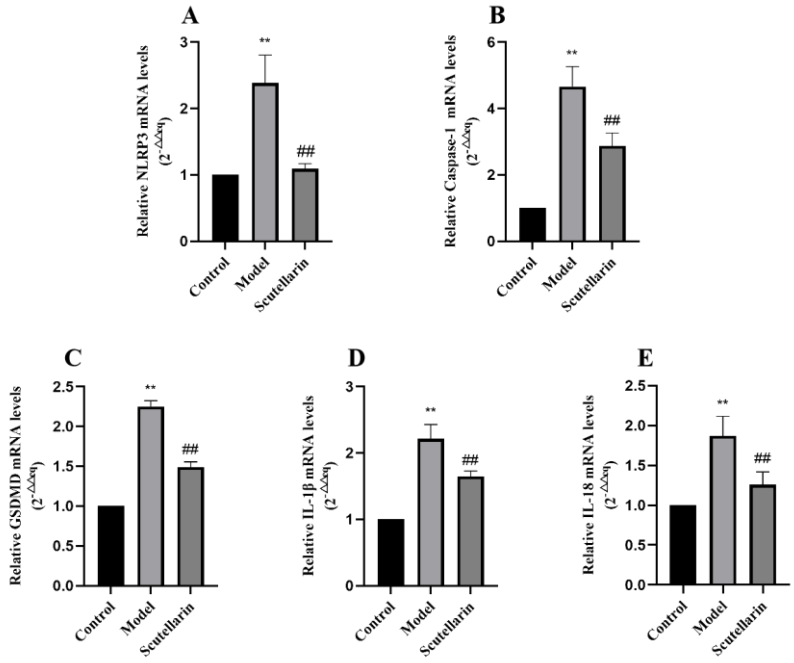

Fig. 4. Effect of scutellarin on the key mRNA expression of the NLRP3/caspase-1/GSDMD signaling pathway in LPS and ATP-induced pyroptosis model cells: a) NLRP3; b) caspase-1; c) GSDMD; d) IL-1β; e) IL-18. Data are presented as mean ± SD ($n = 3$). Compared with control group, $^{**}p < 0.01$; compared with model group, $^{\#\#}p < 0.01$.

Effect of scutellarin on the fluorescence expression of NLRP3 in LPS and ATP-induced pyroptosis model cells

Compared with the control group, the fluorescence expression of NLRP3 in the model group was significantly increased ($p < 0.01$). Compared with the model group, scutellarin reversed the fluorescence expression of NLRP3 ($p < 0.01$) (Fig. 5).

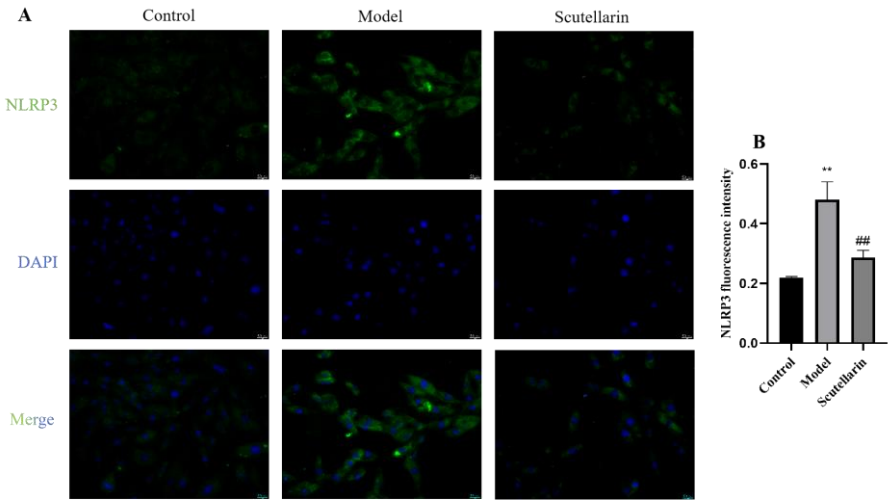

Fig. 5. Effect of scutellarin on the fluorescence expression of NLRP3 in LPS and ATP-induced pyroptosis model cells: a) representative image of NLRP3 fluorescence intensity (20 μm); b) quantitative analysis of NLRP3 fluorescence intensity. Data are presented as mean ± SD (n = 3). Compared with control group, $^{**}p < 0.01$; compared with model group, $^{\#\#}p < 0.01$.

Effect of scutellarin on the fluorescence expression of caspase-1 in LPS and ATP-induced pyroptosis model cells

Compared with the control group, the fluorescence expression of caspase-1 in the model group was significantly increased ($p < 0.01$). Compared with the model group, scutellarin reversed the fluorescence expression of caspase-1 ($p < 0.01$) (Fig. 6).

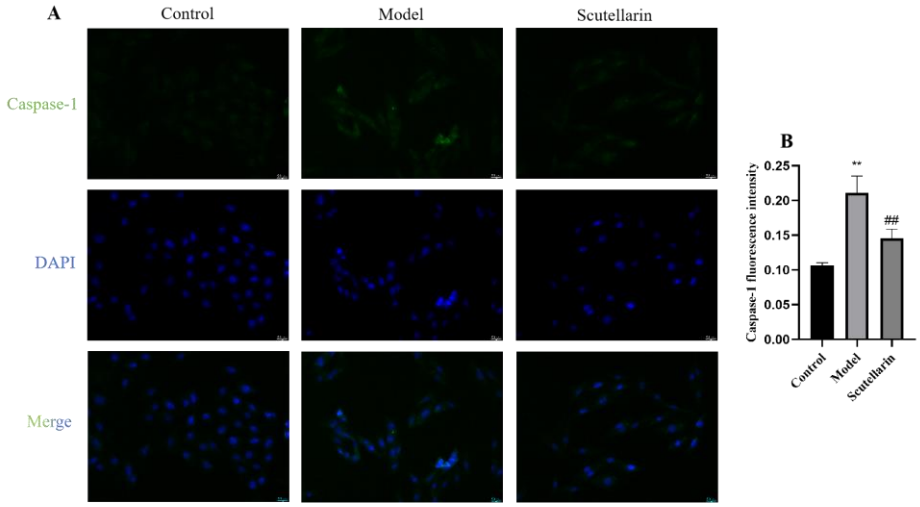

Fig. 6. Effect of scutellarin on the fluorescence expression of caspase-1 in LPS and ATP-induced pyroptosis model cells: a) representative image of caspase-1 fluorescence intensity (20 μm); b) quantitative analysis of caspase-1 fluorescence intensity. Data are

presented as mean ± SD (n = 3). Compared with control group, $^{**}p < 0.01$; compared with model group, $^{\#\#}p < 0.01$.

Effect of scutellarin on the fluorescence expression of GSDMD in H9c2 cells

Compared with the control group, the fluorescence expression of GSDMD in the model group was significantly increased ($p < 0.01$). Compared with the model group, scutellarin reversed the fluorescence expression of GSDMD ($p < 0.01$) (Fig. 7).

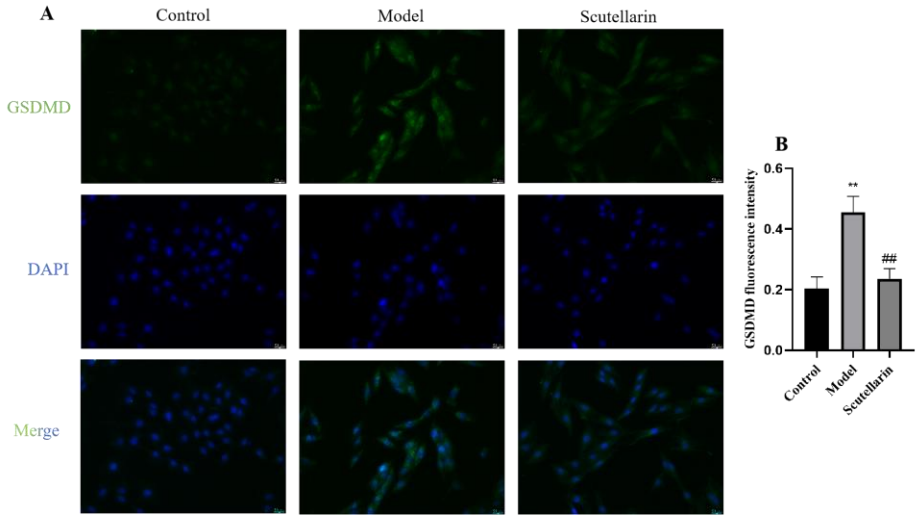

Fig. 7. Effect of scutellarin on the fluorescence expression of GSDMD in LPS and ATP-induced pyroptosis model cells: a) representative image of caspase-1 fluorescence intensity (20 μm); b) quantitative analysis of GSDMD fluorescence intensity. Data are presented as mean ± SD (n = 3). Compared with control group, $^{**}p < 0.01$; compared with model group, $^{\#\#}p < 0.01$.

Effect of scutellarin on the protein expression of NLRP3 in LPS and ATP-induced pyroptosis model cells

Protein expression of NLRP3 was significantly increased in the model group as compared to the control group ($p < 0.05$). Compared with the model group, scutellarin reversed the expression of NLRP3 ($p < 0.05$) (Fig. 8).

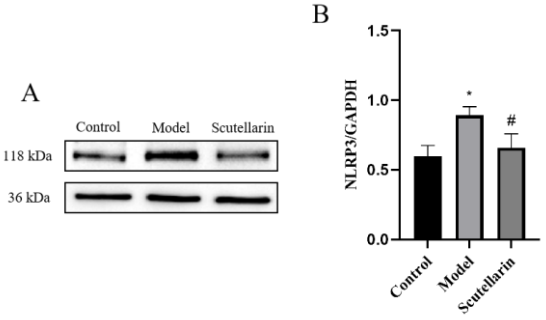

Fig. 8. Effect of scutellarin on the protein expression of NLRP3 in LPS and ATP-induced

pyroptosis model cells: a) protein bands of NLRP3 (118 kDa) and GAPDH (36 kDa); b) NLRP3 protein expression. Data are presented as mean ± SD (n = 3). Compared with control group, $^{*}p < 0.05$, Compared with model group, $^{\#}p < 0.05$.

CONCLUSIONS

Scutellarin can ameliorate myocardial cell damage by down-regulating the NLRP3/caspase-1/GSDMD pathway, reducing the release of IL-1β and IL-18, and improving the inflammatory damage of myocardial cells. In future experiments, we will investigate the inhibition effect of scutellarin using NLRP3 gene overexpression, and fully explain the mechanism of its myocardial protection.

Supporting material is available from the corresponding author upon request.

Conflict of interest. – The authors declared no conflict of interest.

Funding. – This work was supported by The University Synergy Innovation Program of Anhui Province (No.GXXT-2023-073).

Authors contributions. –

REFERENCES

1. S. Toldo and A. Abbate, The role of the NLRP3 inflammasome and pyroptosis in cardiovascular diseases, *Nat. Rev. Cardiol*. **21** (2024) 219–237; https://doi.org/10.1038/s41569-023-00946-3
2. S. Toldo, E. Mezzaroma, L. F. Buckley, N. Potere, M. Di Nisio, G. Biondi-Zoccai, B. W. Van Tassell and A. Abbate, Targeting the NLRP3 inflammasome in cardiovascular diseases; *Pharmacol. Ther*. **236** (2022) Article ID 108053; https://doi.org/10.1016/j.pharmthera.2021.108053
3. C. Pellegrini, A. Martelli, L. Antonioli, M. Fornai, C. Blandizzi and V. Calderone, NLRP3 inflammasome in cardiovascular diseases: Pathophysiological and pharmacological implications, *Med. Res. Rev*. **41** (2021) 1890–1926; https://doi.org/10.1002/med.21781
4. H. Y. Fang, X. N. Zhao, M. Zhang, Y. Y. Ma, J. L. Huang and P. Zhou, Beneficial effects of flavonoids on cardiovascular diseases by influencing NLRP3 inflammasome. *Inflammopharmacol*. **31** (2023) 1715–1729; https://doi.org/10.1007/s10787-023-01249-2
5. J. P. Li, S. Qiu, G. J. Tai, Y. M. Liu, W. Wei, M. M. Fu, P. Q. Fang, J. N. Otieno, T. Battulga, X. X. Li and M. Xu, NLRP3 inflammasome-modulated angiogenic function of

EPC via PI3K/Akt/mTOR pathway in diabetic myocardial infarction, *Cardiovasc. Diabetol*. **24** (2025) 6; https://doi.org/10.1186/s12933-024-02541-3

6. W. Zhou, C. Chen, Z. Chen, L. Liu, J. Jiang, Z. Wu, M. Zhao and Y. Chen, NLRP3: A novel mediator in cardiovascular disease, *J. Immunol. Res*. **2018** (2018) 5702103; https://doi.org/10.1155/2018/5702103
7. J. Fu and H. Wu, Structural mechanisms of NLRP3 inflammasome assembly and activation, *Annu. Rev. Immunol*. **41** (2023) 301–316. https://doi.org/10.1146/annurev-immunol-081022-021207
8. Y. Xie, G. Sun, Y. Tao, W. Zhang, S. Yang, L. Zhang, Y. Lu and G. Du, Current advances on the therapeutic potential of scutellarin: an updated review, *Nat. Prod. Bioprospect*. **14** (2024) 20; https://doi.org/10.1007/s13659-024-00441-3
9. Y. Zhou, C. Gu, Y. Zhu, Y. Zhu, Y. Chen, L. Shi, Y. Yang, X. Lu and H. Pang, Pharmacological effects and the related mechanism of scutellarin on inflammation-related diseases: A review, *Front Pharmacol.* **15** (2024) Article ID 1463140. https://doi.org/10.3389/fphar.2024.1463140
10. X. Zhang, T. Yin, Y. Wang, J. Du, J. Dou and X. Zhang, Effects of scutellarin on the mechanism of cardiovascular diseases: A review, *Front. Pharmacol*. **14** (2024) Article ID 1329969; https://doi.org/10.3389/fphar.2023.1329969
11. L. J. Xu, R. C. Chen, X. Y. Ma, Y. Zhu, G. B. Sun and X. B. Sun, Scutellarin protects against myocardial ischemia-reperfusion injury by suppressing NLRP3 inflammasome activation, *Phytomedicine*. **68** (2020) Article ID 153169; https://doi.org/10.1016/j.phymed.2020.153169
12. H. Sharif, L. Wang, W. L. Wang, V. G. Magupalli, L. Andreeva, Q. Qiao, A.V. Hauenstein, Z. Wu, G. Núñez, Y. Mao and H. Wu, Structural mechanism for NEK7-licensed activation of NLRP3 inflammasome, *Nature* **570** (2019) 338–343; https://doi.org/10.1038/s41586-019-1295-z
13. B. T. Fahr, T. O'Brien, P. Pham, N. D. Waal, S. Baskaran, B. C. Raimundo, J. W. Lam, M. M. Sopko, H. E. Purkey and M. J. Romanowski, Tethering identifies fragment that yields potent inhibitors of human caspase-1, *Bioorg. Med. Chem. Lett*. **16** (2006) 559–562. https://doi.org/10.1016/j.bmcl.2005.10.048
14. S. Kuang, J. Zheng, H. Yang, S. Li, S. Duan, Y. Shen, C. Ji, J. Gan, X. W. Xu, J. Li, Structure insight of GSDMD reveals the basis of GSDMD autoinhibition in cell pyroptosis. *Proc. Natl. Acad. Sci. USA.* **114** (2017) 10642–10647. https://doi.org/10.1073/pnas.1708194114
15. Y. Liu, X. Yang, J. Gan, S. Chen, Z. X. Xiao and Y. Cao, CB-Dock2: improved protein-ligand blind docking by integrating cavity detection, docking and homologous

template fitting. *Nucleic. Acids Res*. **50** (2022) W159-W164. https://doi.org/10.1093/nar/gkac394

16. X. N. Zhao, H. M. Ding, Y. Y. Ma, L. Wang and P. Zhou, Ling-Gui-Zhu-Gan decoction inhibits cardiomyocyte pyroptosis via the NLRP3/Caspase-1 signaling pathway. *Tissue Cell*. **91** (2024) 102588. https://doi.org/10.1016/j.tice.2024.102588
17. X. Chen, Y. Li, J. Li, T. Liu, Q. Jiang, Y. Hong, Q. Wang, C. Li, D. Guo, and Y. Wang, Qishen granule (QSG) exerts cardioprotective effects by inhibiting NLRP3 inflammasome and pyroptosis in myocardial infarction rats. *J. Ethnopharmacol*. **285** (2025) 114841; https://doi.org/10.1016/j.jep.2021.114841
18. Y. Qiu, Y. Huang, M. Chen, Y. Yang, X. Li and W. Zhang, Mitochondrial DNA in NLRP3 inflammasome activation. *Int. Immunopharmacol*. **108** (2022) Article ID 108719. https://doi.org/10.1016/j.intimp.2022.108719
19. N. Kelley, D. Jeltema, Y. Duan and Y. He, The NLRP3 inflammasome: An overview of mechanisms of activation and regulation, *Int. J. Mol. Sci*. **20** (2019) Article ID 3328; https://doi.org/10.3390/ijms20133328
20. Y. Huang, W. Xu and R. Zhou, NLRP3 inflammasome activation and cell death. *Cell Mol. Immunol*. **18** (2021) 2114–2127. https://doi.org/10.1038/s41423-021-00740-6
21. A. Rauf, M. Shah, D. M. Yellon and S. M. Davidson, Role of caspase 1 in ischemia/reperfusion injury of the myocardium, *J. Cardiovasc. Pharmacol*. **74** (2019) 194–200; https://doi.org/10.1097/FJC.0000000000000694
22. B. Zhang, G. Liu, B. Huang, H. Liu, H. Jiang, Z. Hu and J. Chen, KDM3A attenuates myocardial ischemic and reperfusion injury by ameliorating cardiac microvascular endothelial cell pyroptosis, *Oxid. Med. Cell Longev*. **2022** (2022) Article ID 4622520. https://doi.org/10.1155/2022/4622520
23. S. Toldo and A. Abbate, The NLRP3 inflammasome in acute myocardial infarction. *Nat. Rev. Cardiol*. **15** (2018) 203–214. https://doi.org/10.1038/nrcardio.2017.161
24. Y. S. Tang, Y. H. Zhao, Y. Zhong, X. Z. Li, J. X. Pu, Y. C. Luo and Q. L. Zhou, Neferine inhibits LPS-ATP-induced endothelial cell pyroptosis via regulation of ROS/NLRP3/Caspase-1 signaling pathway, *Inflamm. Res*. **68** (2019) 727–738. https://doi.org/10.1007/s00011-019-01256-6
25. E. L. Johnston, B. Heras, T. A. Kufer, and M. Kaparakis-Liaskos, Detection of bacterial membrane vesicles by NOD-like receptors, *Int. J. Mol. Sci*. **22** (2021) 1005. https://doi.org/10.3390/ijms22031005
26. H. Kong, H. Zhao, T. Chen, Y. Song and Y. Cui, Targeted P2X7/NLRP3 signaling pathway against inflammation, apoptosis, and pyroptosis of retinal endothelial cells in diabetic retinopathy. *Cell Death Dis*. **13** (2022) 336. https://doi.org/10.1038/s41419-022-04786-w

27. S. Nie, S. Zhang, R. Wu, Y. Zhao, Y. Wang, X. Wang, M. Zhu and P. Huang, Scutellarin: pharmacological effects and therapeutic mechanisms in chronic diseases, *Front Pharmacol*. **15** (2024) Article ID 1470879; https://doi.org/10.3389/fphar.2024.1470879
28. J. K. Li, Z. P. Song and X. Z. Hou, Scutellarin ameliorates ischemia/reperfusion injury-induced cardiomyocyte apoptosis and cardiac dysfunction via inhibition of the cGAS-STING pathway, *Exp. Ther. Med*. **25** (2023) 155; https://doi.org/10.3892/etm.2023.11854
29. X. Fan, Y. Wang, X. Li, T. Zhong, C. Cheng and Y. Zhang, Scutellarin alleviates liver injury in type 2 diabetic mellitus by suppressing hepatocyte apoptosis *in vitro* and *in vivo*, *Chin. Herb Med*. **15** (2023) 542–548. https://doi.org/10.1016/j.chmed.2023.03.007
30. L. Peng, L. Wen, Q. F. Shi, F. Gao, B. Huang, J. Meng, C. P. Hu and C. M. Wang, Scutellarin ameliorates pulmonary fibrosis through inhibiting NF-κB/NLRP3-mediated epithelial-mesenchymal transition and inflammation. *Cell Death Dis*. **11** (2020) 978. https://doi.org/10.1038/s41419-020-03178-2
31. W. C. Gao, T. H. Yang, B. B. Wang, Q. Liu, Q. Li, Z. H. Zhou, C. B. Zheng and P. Chen, Scutellarin inhibits oleic acid induced vascular smooth muscle foam cell formation via activating autophagy and inhibiting NLRP3 inflammasome activation, *Clin. Exp. Pharmacol. Physiol*. **51** (2024) e13845. https://doi.org/10.1111/1440-1681.13845
32. Z. Wang, P. Zhang, Y. Zhao, F. Yu, S. Wang, K. Liu, X. Cheng, J. Shi, Q. He, Y. Xia and L. Cheng, Scutellarin protects against mitochondrial reactive oxygen species-dependent NLRP3 inflammasome activation to attenuate intervertebral disc degeneration, *Front. Bioeng. Biotechnol*. **10** (2022) 883118. https://doi.org/10.3389/fbioe.2022.883118
33. H. T. Bian, G. H. Wang, J. J. Huang, L. Liang, L. Xiao, and H. L. Wang, Scutellarin protects against lipopolysaccharide-induced behavioral deficits by inhibiting neuroinflammation and microglia activation in rats, *Int. Immunopharmacol*. **88** (2020) Article ID 106943. https://doi.org/10.1016/j.intimp.2020.106943